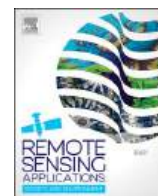


Contents lists available at [ScienceDirect](https://www.sciencedirect.com)

Remote Sensing Applications: Society and Environment

journal homepage: www.elsevier.com/locate/rsase

Spatio-temporal variability of pelagic *Sargassum* landings on the northern Mexican Caribbean

Rosa E. Rodríguez-Martínez^{a,*}, Eric Jordán-Dahlgren^a, Chuanmin Hu^b

^a Unidad Académica de Sistemas Arrecifales-Puerto Morelos, Instituto de Ciencias del Mar y Limnología, Universidad Nacional Autónoma de México, Puerto Morelos, Quintana Roo, 77580, Mexico

^b College of Marine Science, University of South Florida, 140 Seventh Avenue South, St. Petersburg, FL, 33701, USA

ARTICLE INFO

Keywords:

Macroalgal blooms
Wrack deposition
Beach monitoring
Satellite image data

ABSTRACT

The massive influx of pelagic *Sargassum* (sargasso) has produced environmental, socio-economic, and human health-related problems in several Atlantic countries in the last decade. Predicting sargasso landings to areas of interest is necessary to implement management actions. To date, quantitative assessments of beach-cast volumes are scarce, making it challenging to test prediction models based on remote sensing measurements and environmental variables. In this study, we analyze the variability in sargasso beach-cast accumulation in the northern Mexican Caribbean coast in 2018 and 2019 and its relationship with: (1) wind direction and speed, (2) sea surface temperature, and (3) sargasso biomass measured with MODIS in the southwestern Caribbean Sea and the Mexican Caribbean exclusive economic zone. We use data on the monthly volume of sargasso removed from the beach by seven hotels over a 40 km section of shoreline. The mean monthly volume per kilometer of shoreline was higher in 2018 (1852 m³), but that of 2019 was also significant (1773 m³). Landing patterns were variable, with the peak months differing among sites within years and years within sites. High-volume stranding lasted seven months in 2018 and five in 2019. In both years, high beaching occurred during the summer when the wind direction was between 90° and 180° with wind speeds of 4–8 m s⁻¹. The mean volume in the record-breaking month of 2019 (May = 6565 m³ km⁻¹) was more significant than the highest of 2018 (June = 3816 m³ km⁻¹). MODIS data and landing volumes showed a similar seasonal pattern, but maximum satellite signals occurred at different months than those with maximum beaching. We found a significant ($p < 0.05$) but low correlation (Kendall tau < 0.3) between the volume of sargasso washing ashore and in situ sea surface temperature (SST), and no meaningful relationship between SST measured by MODIS and (1) sargasso abundance measured by MODIS and (2) sargasso landing volumes. The information reported in this study can help to test forecasting models and is valuable for sargasso management and valorization.

1. Introduction

Macroalgae blooms have increased worldwide in recent years with those of the genera *Ulva* and *Sargassum* being the most prominent worldwide (Smetacek and Zingone, 2013; Xiao et al., 2020). Since 2011, pelagic *Sargassum* species (*S. fluitans* and *S. natans*; from now on sargasso) have increased in abundance in the Atlantic Ocean and inundated coastlines in West Africa, northern Brazil, and

* Corresponding author.

E-mail address: rosaer@cmarl.unam.mx (R.E. Rodríguez-Martínez).

<https://doi.org/10.1016/j.rsase.2022.100767>

Received 24 August 2021; Received in revised form 22 March 2022; Accepted 27 April 2022

Available online 14 May 2022

2352-9385/© 2022 Elsevier B.V. All rights reserved.

the Caribbean producing socio-economic and environmental problems (Gower et al., 2013; Smetacek and Zingone, 2013; Franks et al., 2016; van Tussenbroek et al., 2017; Rodríguez-Martínez et al., 2019; Wang et al., 2019). Satellite observations allowed the identification of the great Atlantic *Sargassum* belt, extending for eight thousand kilometers from the west coast of Africa to the Gulf of Mexico (Wang et al., 2019). Hypotheses on the causes of the increments in sargasso biomass include increases in sea surface temperature (Johns et al., 2020) and nutrient load to the Atlantic (Wang et al., 2019), abnormal wind regimes from 2009 to 2010 in the central-eastern Atlantic (Johns et al., 2020), a change in upwelling patterns off the northeastern coast of Africa and the open ocean (Sissini et al., 2017; Wang et al., 2019), a change in the dispersion patterns of the Sahara dust (Johnson et al., 2013), or the result of these causes together (Johns et al., 2020).

The first massive influx of sargasso in the Mexican Caribbean began in late 2014, reaching higher landings in September 2015 (Rodríguez-Martínez et al., 2016). Sargasso influx decreased significantly in 2016 and 2017 but increased again in February 2018 and continued until September 2019. Massive sargasso landings to this region have resulted in mortality of seagrass meadows (van Tussenbroek et al., 2017) and marine fauna (Rodríguez-Martínez et al., 2019) and enhanced beach erosion (Chávez et al., 2020). It has also affected the tourism industry, a significant source of income for this region (Chávez et al., 2020). Another potential impact is the accumulation of toxic elements (e.g., arsenic, copper, and cadmium) imported by sargasso into beaches and nearshore waters (Rodríguez-Martínez et al., 2020; Vázquez-Delfín et al., 2021).

The massive beaching of sargasso is potentially becoming “the normal” on this coast. Its impacts on susceptible areas demand reliable forecasting tools and practical management actions. Significant research has focused on monitoring Atlantic sargasso blooming events in the open ocean through remote sensing (Wang et al., 2019; Trinanes et al., 2021; Wang and Hu, 2021). Unfortunately, currently used platforms have spatial and temporal resolution limitations that prevent near real-time beach monitoring. Also, the variability in the state of organic decomposition and water content in sargasso leads to a significant variation in spectral reflectance (López-Conteras et al., 2021).

In situ monitoring of sargasso landings have been few and limited in space and time. For example, Fidai et al. (2020) conducted a literature search to identify sargasso monitoring research from 1960 to 2019 and found that only twelve publications measured beach cast volumes. More recently, three other studies quantified pelagic sargasso beach cast volumes for small (<1 km) sections of the coast, one conducted in the eastern littoral of Havana (Torres-Conde and Martínez-Daranas, 2020) and two in the Mexican Caribbean coast (García-Sánchez et al., 2020; Vázquez-Delfín et al., 2021). Only one study has analyzed the relationship between sargasso abundance measured from remote sensing imagery and beach cast volumes (Tomenchok et al., 2021).

Quantitative data on sargasso landings is necessary to understand the variability in space and time and their relationship with environmental factors. It is also needed to prioritize areas to attend to, determine the resources required to conduct proper management, and estimate the potential biomass to industrialize. To increase our understanding of these macroalgal bloom events, the goals of this study were to analyze (1) the Spatio-temporal variability in sargasso landing volumes in the northern Mexican Caribbean coast, (2) the relationship between depositional volumes with wind speed and direction and sea surface temperature, and (3) the relationship between sargasso coverage measured from satellite imagery and the volume of sargasso landings to this coast. The information provides a baseline on the abundance of sargasso on recipient beaches. It could also help test models intended to provide advanced warnings of arrival dates of large masses of sargasso and estimate potential volumes for industrialization.

2. Method

2.1. Study sites

The study was conducted in a beach sector located in the northern sector of the Mexican Caribbean coast (Fig. 1A). The sargasso masses that land on this coastline are presumed to be transported by the Yucatan Current, a significant Caribbean Current branch,

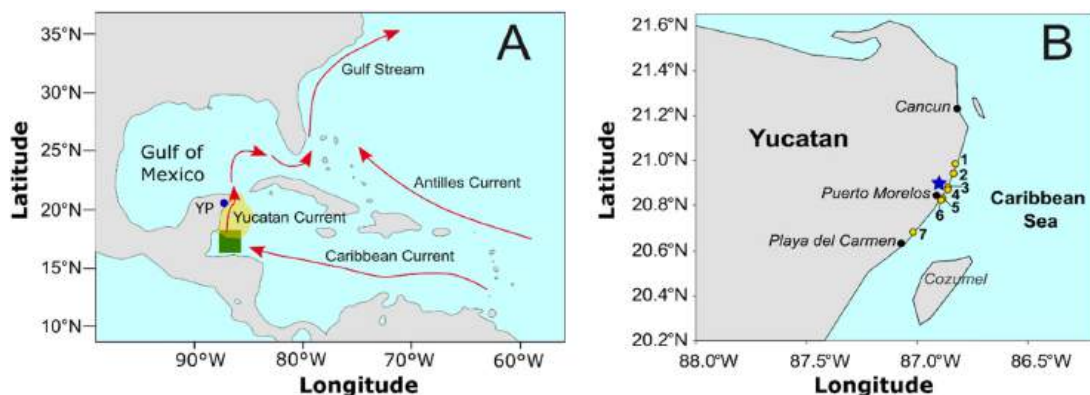


Fig. 1. (A) Location of study site in the NE Yucatan Peninsula (YP) and areas used to measure oceanic sargasso biomass from satellite imagery in the SW Caribbean (green square) and the Exclusive Economic Zone of Mexico in the Caribbean (yellow shape); (B) Location of hotels (numbers 1–7) that monitored the monthly volume of sargasso removed from the beach in 2018 and 2019 and of the Oceanographic and Meteorology Monitoring Service of UNAM (blue star). (For interpretation of the references to colour in this figure legend, the reader is referred to the Web version of this article.)

which has a direction that fluctuates northeastward to northwestward and a mean velocity of 5.4 km h^{-1} near the surface (Candela et al., 2003).

The wind regime also plays a role in the quantity of sargasso landing; east and southeast winds favor the movement of sargasso towards the land during spring and summer, whereas northerly winds inhibit onshore transport during autumn and winter (García-Sánchez et al., 2020). Prevailing sea wind direction and speed data obtained daily at 10-min intervals for 2018 and 2019 were provided by the Oceanographic and Meteorology Monitoring Service of UNAM in Puerto Morelos (see location in Fig. 1), which has an ISO 9001 certification (SAMMO, 2020). Wind speed during the study period ranged from 0 to 15.7 m s^{-1} , with means of 5.2 and 4.3 m s^{-1} in 2018 and 2019, respectively. In both years, the dominant winds came primarily from the east to the southeast, with a more significant proportion of winds from the southeast in 2019 (Fig. 2). A notable proportion of winds came from the northeast and south; winds from the north and northwest were least frequent (Fig. 2). During the study period, Sea surface temperature ranged from 25.3 to $30.9 \text{ }^\circ\text{C}$ (SAMMO, 2020).

2.2. In situ estimation of sargasso beach cast volumes

Volumetric data on the amount of beached sargasso removed in 2018 and 2019 was provided by seven hotels that collectively account for 6.93 km of sampling distance over a 40 km section of shoreline (Fig. 1B). The beach length at the study sites ranged from 0.2 to 2.2 km (Table 1). Sites 1–4 are protected by a coral reef barrier, while sites 5–7 are exposed to the ocean waves. Hotels have different strategies to remove the algae from the beach, depending on beaching volumes, beachfront length, human and economic resources, method of collection, and availability of disposal sites within their property. Manual harvesting methods were preferred over mechanical when the beaching volumes allowed it to prevent erosion. Hotels clean their beachfront on a near-daily basis, but they report the data differently. In three hotels (1, 2, and 5), the daily volume was recorded based on the number of trips made by rakes or trucks of known capacity (7 m^3 or 14 m^3) to move the sargasso to an area within their property. The rest of the hotels provided data based on their accountability reports regarding the cost of the total number of trucks rented to transport the algae to disposal sites outside their property. Due to significant differences in beachfront lengths, the volumetric data were standardized as cubic meters per kilometer ($\text{m}^3 \text{ km}^{-1}$).

The material removed from the beach was mainly pelagic *Sargassum* spp. (*S. fluitans* III, *S. natans* I, and *S. natans* VIII); however, it could also include sand, seagrasses, and occasionally other macroalgae. The proportion of these components was variable, depending on collection methods, wave energy, and extension of seagrass beds. However, during the higher landing months, the main element (>85%) was sargasso (see Supplementary Fig. 1). Sampling areas on each study site were the same in the two sampling years.

2.3. Estimation of sargasso biomass and sea surface temperature from satellite imagery

Sargasso distributions maps were derived from the Moderate Resolution Imaging Spectroradiometer (MODIS/Aqua and MODIS/Terra) satellite measurements using algorithms detailed in Wang and Hu (2016) (for areal density or % cover estimates) and Wang et al. (2018) (for biomass density estimates). Briefly, for the study region of the western Caribbean Sea, each MODIS pixel ($\sim 1 \text{ km}$ resolution) was classified to be no observation (either due to no satellite coverage or the pixel is not interpretable due to clouds, sun glint, or other artifacts), algae containing (here, “algae” refers to sargasso), or algae-free based on the pixel’s reflectance spectral shape and magnitude. The algae content (either % cover or biomass) of the algae-containing pixel was estimated from its red-edge reflectance (e.g., reflectance in the near-infrared). Then, the study region was divided into $0.1^\circ \times 0.1^\circ$ grids, and in each grid, the mean density

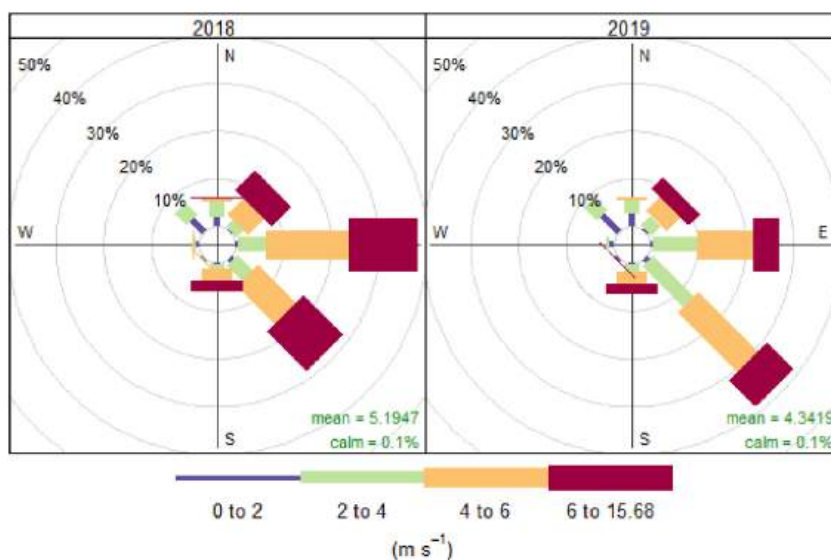


Fig. 2. Windrose plots of mean wind speed and direction frequencies in 2018 and 2019 in the northeastern Mexican Caribbean. Wind speeds are split into the intervals shown by the scale at the bottom of both panels. The grey circles show the percent frequencies.

Table 1

Summary of the amounts of sargasso removed from seven Mexican Caribbean beaches during 2018 and 2019. Beach length is provided for each site. The last two columns show the volume and month of higher landings (peak). For confidentiality reasons, we will not name hotel sites. 95% confidence intervals were estimated using bootstrap resampling.

Hotel ID	Beach length (km)	Annual volume (m ³) of sargasso ^a removed		Mean monthly volume (m ³) of sargasso ^a removed per kilometer (95% CI)		Sargasso ^a volume (m ³) removed per kilometer during the peak month	
		2018	2019	2018	2019	2018	2019
1	2.20	90,051	131,639	3316 (1912–5427)	4888 (2002–8674)	13,125 (Jun)	19,470 (May)
2	1.00	22,300	13,211	1863 (1418–2246)	1096 (621–1607)	2661 (Jul)	2993 (May)
3	0.86	12,375	6086	1195 (717–1706)	585 (300–920)	2641 (Aug)	1660 (Jul)
4	0.20	2940	1561	1221 (760–1738)	642 (245–1138)	2925 (Mar)	2415 (Apr)
5	0.60	17,983	15,603	2492 (1723–3247)	2144 (1119–3342)	4480 (May)	5507 (May)
6	0.37	5894	6773	1313 (806–1939)	1433 (390–3286)	3897 (Mar)	10,443 (May)
7	1.70	29,538	28,396	1445 (975–1930)	1376 (628–2278)	2685 (Aug)	4431 (May)

^a Could also include sand, seagrasses, and occasionally other macroalgae.

within a week was estimated from all pixels falling in that grid and during that week. The mean monthly density in each grid was estimated as the arithmetic average of all weekly means in the grid, with standard deviation also calculated. Such derived mean monthly density maps are presented in Fig. 3. The mean wet biomass in a grid was estimated as a product of the mean density and the grid's area and a conversion factor of 3.34 kg m⁻² (Wang et al., 2018). The total sargasso biomass within each region of interest (ROI) is an integration of biomass from all grids in the ROI.

Two ROIs were selected to examine the sargasso temporal patterns in 2018 and 2019: the Southwestern Caribbean Sea (16°–18°N and 85–87°W) and the exclusive economic zone of Mexico in the Caribbean (87.5–84.5°W and 18–21°N) (Fig. 1). These areas were selected because they were the more likely ones from where sargasso can be transported to the study sites. Considering an average surface speed of the Yucatan current of 5.4 km h⁻¹, the sargasso aggregations detected by MODIS in both areas would take up to four days to arrive at the seven beach sites where in situ measurements were made. Ideally, high-resolution satellite images should be used to estimate the sargasso amount near the hotel beaches rather than using coarse-resolution MODIS images to estimate the sargasso amount far away from the beaches. However, high-resolution images such as those from Landsat or Sentinel are not available as often as MODIS images and thus difficult the obtention of continuous time-series data. On the other hand, a case study over the east coast of Florida indicated that *Sargassum* accumulations on beaches were highly correlated to MODIS-based estimates far away from the beaches (Tomenchok et al., 2021), thus justifying the use of MODIS observations here. Monthly sea surface temperature (SST) averages for 2018–2019 were obtained for the two ROIs from the MODIS daytime dataset via NASA's Ocean Color Giovanni data portal.

2.4. Data analysis

Sargasso beaching volumes and biomass measured from satellite imagery are presented as the mean and standard deviation (SD). Since data were non-normal distributed, statistical comparisons on landing volumes among sites for each year were made using Kruskal-Wallis tests and those between years within sites using the Wilcoxon test. The Kolmogorov-Smirnov test was used to assess the significance of the difference between the yearly distribution of sargasso biomass measured from satellite images and the volume of sargasso removed from each study beach. Kolmogorov-Smirnov tests were done with proportional data to allow for equivalent scaling. Kendall's rank correlation coefficient (tau) was used to analyze the relationship between (1) daily sargasso landing volumes at three sites (1, 2, and 5) and local SST, (2) sargasso abundance and SST measured in the two oceanic regions of interest (ROIs) from satellite images, and (3) daily sargasso landing volumes and SST measured in the two ROIs. These analyses were done for each year. The Openair package for R (Carslaw and Ropkins, 2021) was used to produce wind rose plots and to elucidate the effect of wind direction on the abundance of beach cast sargasso. For this analysis, we used data of daily volumes reported by the three hotels that monitor daily beachcast volumes (sites 1, 2, and 5).

All analyses were done in R 4.0.5 (R Core Team, 2021) using packages: dplyr (Wickham et al., 2021), ggpubr (Kassambara, 2020), ggplot2 (Wickham, 2016), pgirmess (Giraudoux, 2013), and tidyr (Wickham, 2021). A reproducible record of all statistical analyses and underlying data is available on GitHub (<https://github.com/rodriguezmtz/VarSarLandings>).

3. Results

3.1. Temporal variability in the volume of *Sargassum* beaching

In 2018, massive sargasso landings started in February, when the mean volume removed per kilometer of beach was 1498 m³ (SD: 844) (Fig. 4). Beach cast volumes raised over time until June when the mean volume peaked (3816 m³ km⁻¹, SD: 4233) and remained above the mean value for the whole study period (1813 m³ km⁻¹) from July to September. From October to March 2019, the mean volume decreased to less than 1150 m³ km⁻¹ but increased again in April 2019, reaching a maximum of 6565 m³ km⁻¹ (SD: 6458) by May 2019. Landings remained high until August (1663 m³ km⁻¹, SD: 2143), lessening afterward until they stopped in November (Fig. 4).

Overall, the total annual volume of sargasso removed from the seven surveyed sites was higher in 2019 (203,269 m³) than in 2018 (181,081 m³), but the mean monthly value was higher in 2018 (1852 m³ km⁻¹; SD: 1712) than in 2019 (1773 m³ km⁻¹; SD: 3035). Higher total values in 2019 resulted mainly from the considerably high landing volumes on site 1, which were 46% higher than those

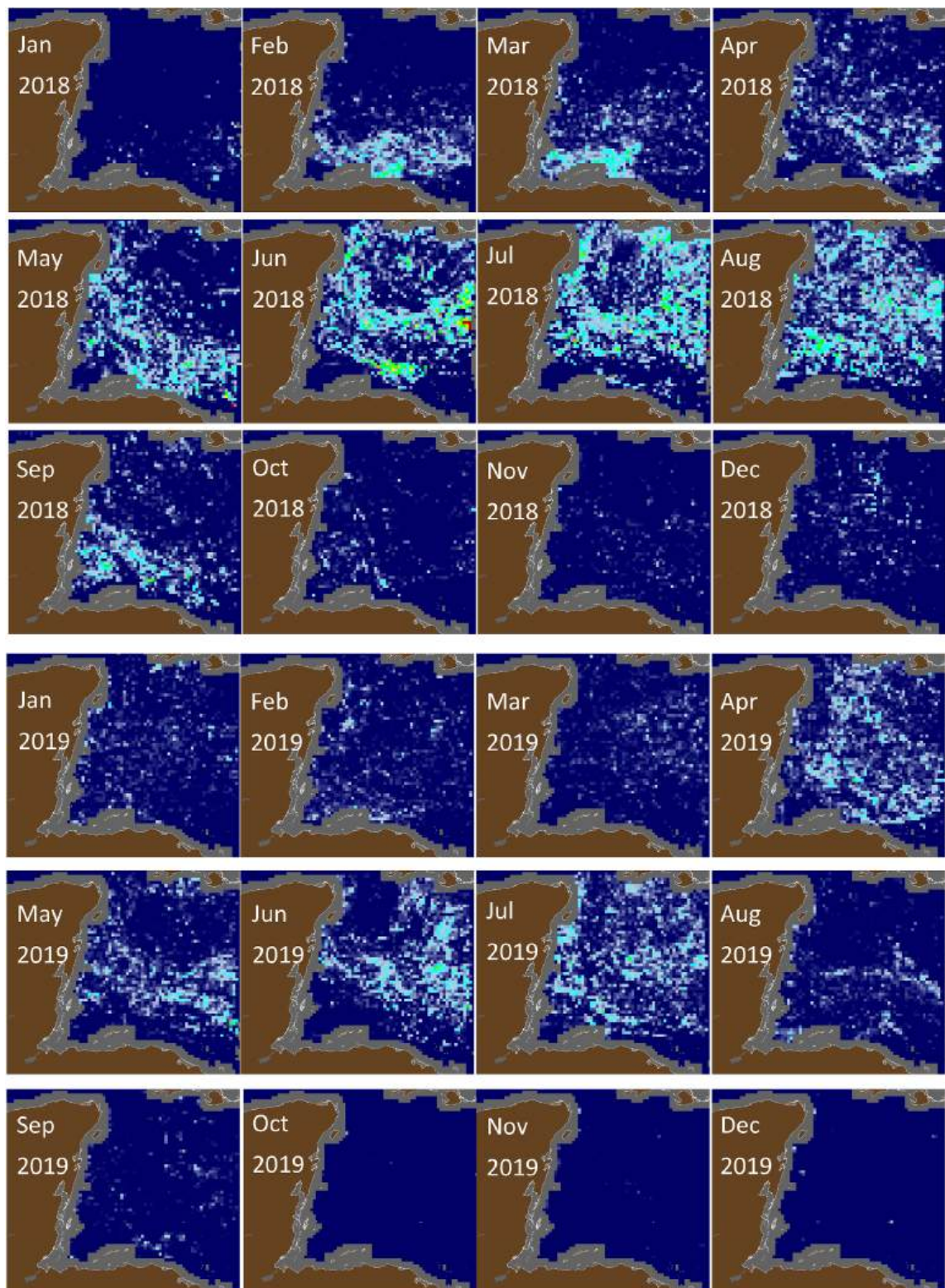


Fig. 3. Monthly mean *Sargassum* density (% cover) in the western Caribbean Sea in 2018 and 2019, derived from MODIS satellite observations using the approach of Wang and Hu (2016).

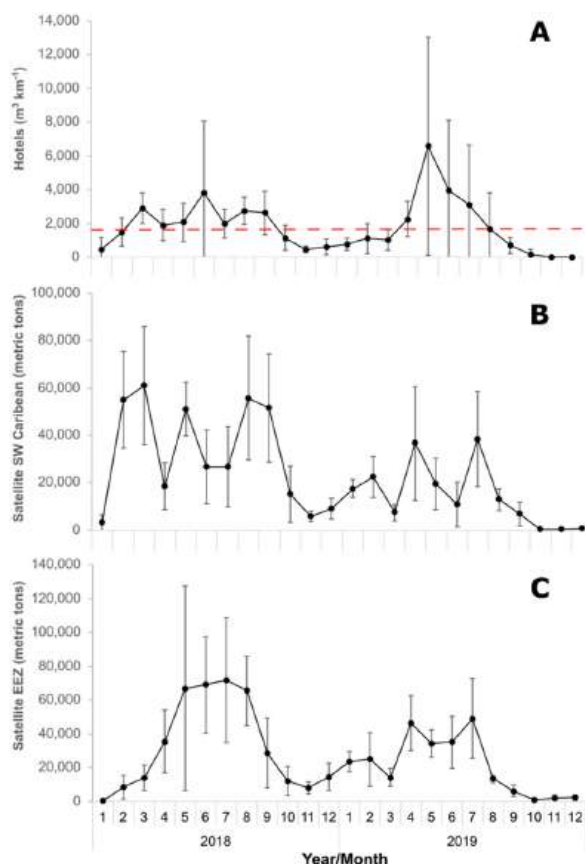


Fig. 4. (A) Mean (\pm SD) volume of sargasso (m^3) removed in 2018 and 2019 from the beachfront of seven hotels in the northern Mexican Caribbean. The red line indicates the mean value for the whole study period ($1812.7 \text{ m}^3 \text{ km}^{-1}$). Sargasso biomass (metric tons) measured from satellite imagery in: (B) the southwestern (SW) Caribbean (from 16 to 18°N and 85 – 87°W), and (C) Mexico's exclusive economic zone (EEZ) in the Caribbean. (For interpretation of the references to colour in this figure legend, the reader is referred to the Web version of this article.)

recorded in 2018. Compared to the other sites, site 1 received nearly double sargasso in 2018 and at least three times more in 2019 (Table 1). Only one other site (6) received higher (15%) total amounts of sargasso in 2019 than in 2018; the rest received between 4 and 51% more sargasso in 2018. The high total values recorded in sites 1 and 6 in 2019 were mainly influenced by atypical high landing volumes in the month of May (Fig. 5). Throughout the monitoring period, mean beach-cast volumes more elevated than the mean value for the study period occurred from March to September 2018 and from April to July 2019 (Fig. 4); thus, the period of high volume strandings was longer in 2018.

Landing patterns were inconsistent across all seven study sites, with peak volumes and months differing among sites within years and years within sites, suggesting episodic landings of large sargasso rafts (Table 1; Fig. 5). The mean monthly landing volumes ranged among sites from 1195 to $3316 \text{ m}^3 \text{ km}^{-1}$ in 2018 and 585 to $4888 \text{ m}^3 \text{ km}^{-1}$ in 2019, and the peak monthly values from 2641 to $13,125 \text{ m}^3 \text{ km}^{-1}$ in 2018, and 1660 to $19,470 \text{ m}^3 \text{ km}^{-1}$ in 2019 (Table 1). The peak months varied among sites from March to August in 2018, while in 2019, five of the sites received the higher quantities in May (Table 1).

In 2018, differences in beach-cast volumes among sites were statistically significant (Kruskal-Wallis test, $H = 14.90$, $df = 6$, $p = 0.0210$), with beaches 1 and 5 receiving significantly higher quantities than 3, 4, and 6 (Wilcoxon test, $p < 0.05$); beach 1 also received significantly higher amounts than beach 7 (Fig. 5). In 2019, beaches 1 and 5 also received more significant amounts than the other five sites. Still, the differences were not statistically significant (Kruskal-Wallis test, $H = 12.11$, $df = 6$, $p = 0.0595$) due to the high variability among months, particularly in site 1 that showed high asymmetry in data distribution. In 2019, this site exhibited four consecutive months of landings higher than those recorded on the other sites (except in May in site 6). For the remaining eight months, beaching volumes in site 1 fell within the range of the other sites. Statistical comparisons between years in the mean annual volume of beach cast sargasso removed from each site showed that only one site (4) received significantly higher amounts in 2018 than in 2019 (Wilcoxon test, $p < 0.05$) (Fig. 5).

3.2. Satellite vs. *in situ* measurements

Sargasso was recorded by satellite images in the two selected regions all year long in both study years (Fig. 2). The maximum sargasso signals in the southwestern region covered February–September 2018 and April–July 2019. Top coverages were recorded in

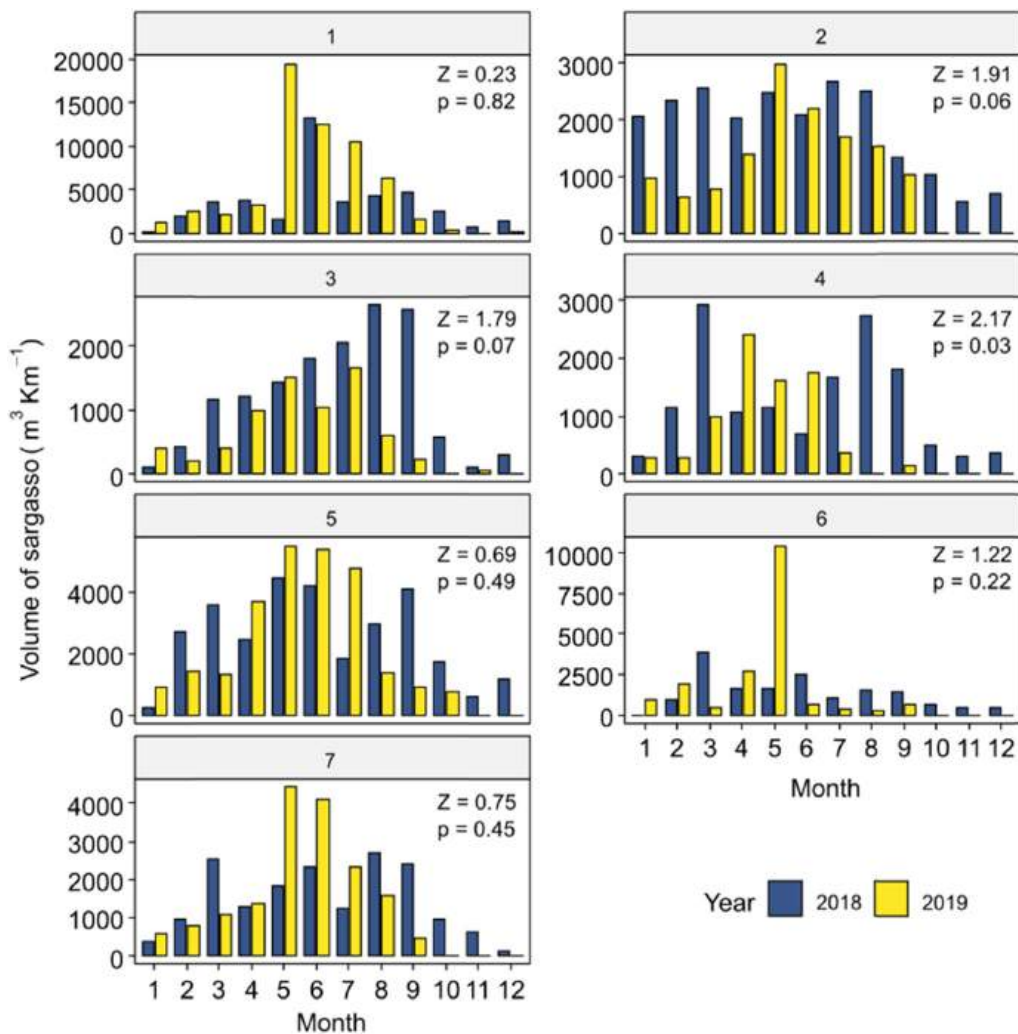


Fig. 5. Volume of beach cast sargasso ($m^3 km^{-1}$) removed monthly from seven tourist beaches in the northern sector of the Mexican Caribbean coast in 2018 and 2019. Numbers above each plot indicate the study site. Results of the Wilcoxon test between years appear in the upper corner of each plot.

the exclusive economic zone in May–August 2018 and April–July 2019. The mean biomass of sargasso during the peak months was higher in 2018 than in 2019 in the two study regions (Fig. 4B and C).

The plots on the mean monthly volume of sargasso (m^3) removed from the beach by hotels (Fig. 4A) and those on sargasso biomass (metric tons) measured from satellite images (Fig. 4B and C) show similar seasonal patterns. The results of the Kolmogorov-Smirnov test revealed no significant differences in the distribution of pairwise distances between sargasso beach cast volume data for each of the seven study beaches and sargasso biomass measured from satellite images (Table 2). Thus, a positive relationship was identified

Table 2

Kolmogorov-Smirnov tests result for the comparison in the distribution of pairwise distances between sargasso biomass measured from satellite images in the SW Caribbean and the Exclusive Economic Zone (EEZ) of Mexico in the Caribbean and beach cast volume data for each of the seven study beaches in 2018 and 2019.

Site	SW Caribbean				EEZ			
	2018		2019		2018		2019	
	D	p	D	p	D	p	D	p
1	0.33	0.54	0.25	0.87	0.25	0.87	0.25	0.87
2	0.42	0.26	0.25	0.85	0.33	0.54	0.25	0.85
3	0.17	1.00	0.17	1.00	0.17	1.00	0.17	1.00
4	0.25	0.85	0.33	0.52	0.17	1.00	0.33	0.52
5	0.17	1.00	0.25	0.85	0.17	1.00	0.25	0.85
6	0.25	0.85	0.42	0.25	0.25	0.85	0.42	0.25
7	0.17	1.00	0.25	0.85	0.33	0.54	0.25	0.85

between the “source” sargasso areas and landing volumes on beaches. However, the maximum sargasso signals detected from satellite images occurred in different months than those with maximum beaching.

Biomass measurements made in situ show that the mean beach cast during the peak months was higher in 2019 than in 2018, whereas those made from satellite images show higher volumes in the peak months of 2018 (Fig. 4). This difference is influenced by the high landings on site 1, which annually receives considerably more significant amounts of sargasso than the other six sites and was particularly affected in 2019, especially in May, when almost 20,000 m³ landed (Fig. 5).

3.3. Relation to environmental conditions

Daily data on sargasso beach cast volumes from three sites (1, 2, and 5) were used to produce plots to elucidate the effect of wind direction (Fig. 6). Wrack volume was higher when the wind direction was between 90° and 135°, representing 61% and 46% of the total amount recorded in 2018 and 2019. In 2019, winds from 135° to 180° also accounted for a high percentage (40%) of landings. In both years, sargasso landings of lower magnitude occurred when the winds were from the northeast and southwest; almost no sargasso (<1%) landed when the wind came from 225° to 45°. The larger quantities of sargasso landed when wind speed ranged from 4 to 8 m s⁻¹.

We found a significant but low correlation ($p < 0.05$) (Kendall tau = 0.22 in 2018 and 0.09 in 2019) between the daily volume of sargasso that landed at sites 1, 2, and 5 and in situ sea surface temperature in the two study years (Supplementary Table 1). No significant correlation ($p > 0.05$) was found between sargasso biomass and SST measured from satellite images in the southwestern Caribbean (Kendall tau = 0.12 in 2018 and -0.33 in 2019) or the Exclusive Economic Zone of Mexico in the Caribbean (Kendall tau = 0.33 in 2018 and -0.24 in 2019) (Supplementary Table 1). In both in situ (Fig. 7) and satellite image measurements (Supplementary Fig. 2), the highest abundance of sargasso occurred before the period of most elevated temperatures.

4. Discussion

4.1. Sampling strategies and uncertainties

Hotels usually remove all the beach cast material from their beach fronts daily; however, on occasions, sargasso landing volumes surpass their clean-up capacity, so some of the values reported can be underestimated. Conversely, some sargasso volumes might be overestimated as the material removed from the beach could also include other components whose proportion can be variable in time and space. For example, beach cast seagrasses tend to be more abundant in sites facing vast coral reef lagoons, especially after the formation of sargasso-brown-tides, when those close to shore die. Also, sand tends to become more attached to blades when wave breaking is more energetic. Finally, reported volume values could be variable due to differences in the timing and method of collections, amount of water and sand retention, degree of compaction, and the time elapsed until their transportation to disposal sites. Nevertheless, given the lack of quantitative data of sargasso on beaches, the data from hotel removals may represent a reliable source for quantitative estimation.

Indeed, our results on sargasso landing volumes to seven beaches along the northern Mexican Caribbean are consistent with reports regarding 2018 as a record-breaking year concerning sargasso biomass reaching Caribbean shores (Wang et al., 2019). Nevertheless, landing volumes during the summer months of 2019 were also significant. In 2018, there was a more prolonged interval of extensive volume strandings (March to September) than in 2019 (April to July). However, even though sargasso beach cast biomass in most sites

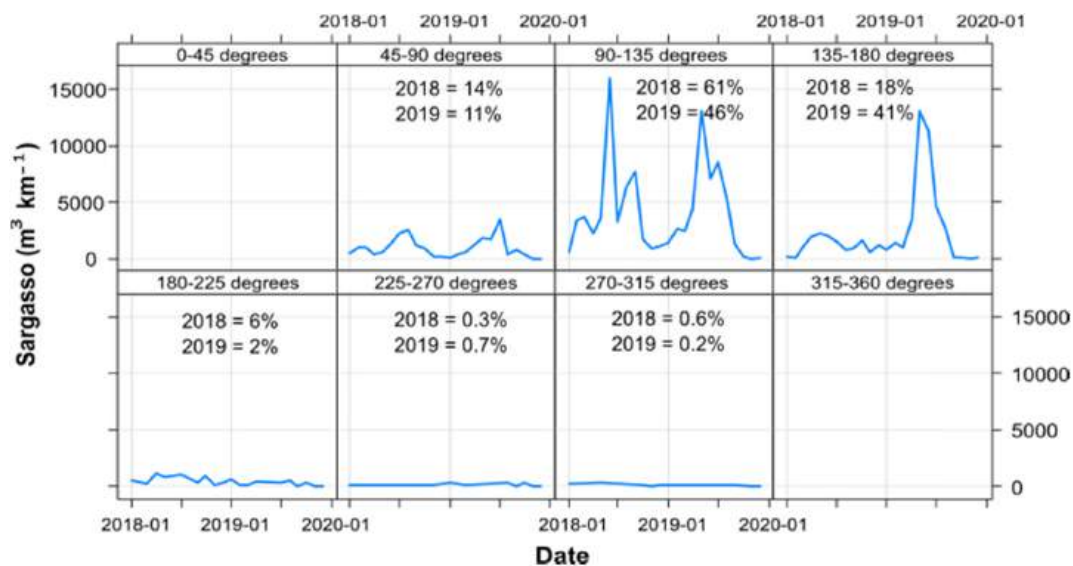


Fig. 6. Relation between wind direction and the mean monthly volume of sargasso removed from three beaches (Sites 1, 2, and 5) in the northern Mexican Caribbean in 2018 and 2019. The percentages of landing volumes that occurred at each wind direction range each year are shown inside each box.

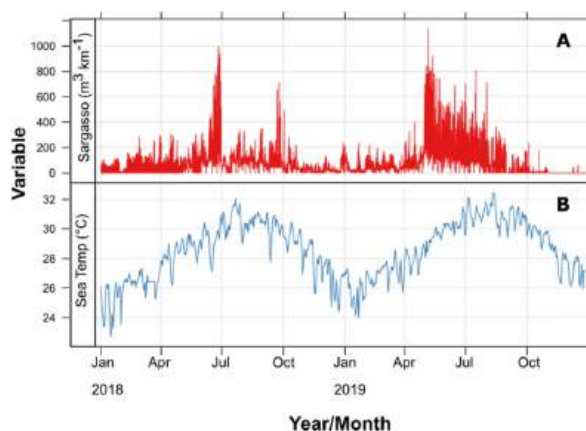


Fig. 7. Time series for the mean daily volume of (A) beach-cast sargasso ($\text{m}^3 \text{km}^{-1}$) removed from three beach sites (1, 2, and 5), and (B) sea surface temperature ($^{\circ}\text{C}$) recorded in the northern Mexican Caribbean in 2018 and 2019.

and months was higher in 2018 than in 2019 (Fig. 4), the mean volume that landed during the peak month of 2019 (May = $6403 \text{ m}^3 \text{km}^{-1}$) was greater than that of 2018 (June = $3699 \text{ m}^3 \text{km}^{-1}$). The peak volumes recorded in these two years were higher than those for the same beach sector in 2015 (September = $2360 \text{ m}^3 \text{km}^{-1}$; Rodríguez-Martínez et al., 2016). The higher in situ volumes recorded in the peak months of 2019, were influenced by the high biomass that landed in two sites (1 and 6), particularly in May.

The studies about pelagic sargasso landing quantities are few and usually employ different sampling units. To compare our results with those from other studies, we use the mean mass-to-volume value ($276 \text{ kg}\cdot\text{m}^{-3}$) and the mean wet-to-dry weight conversion factor (8.49) provided by Salter et al. (2020). By doing this, we obtain mean monthly landing values per kilometer of the beach of 524 and 497 tons of wet weight, or 45 and 42 tons of dry biomass, for 2018 and 2019, respectively. The mean wet biomass recorded in 2018 is similar to that reported by García-Sánchez et al. (2020) for the same year along a $\sim 650 \text{ m}$ stretch of coast in Puerto Morelos, Mexico (mean wet biomass; daily = 17.3 kg m^{-2} or monthly = 519 tons km^{-1}). However, landing volumes to this region are lower than those recorded along the Atalaia beach on the northern Brazilian coast in 2015. According to Sissini et al. (2017), in a single day (May 9th) of 2015, 614 wet tons of pelagic sargasso landed per kilometer of this beach. In the present study, the greater volume removed in a single day from one site was almost half ($1135 \text{ m}^3 \text{km}^{-1}$ or 313 tons km^{-1}). In 2018, however, at least one beach in Mexico received sargasso quantities like those recorded in Brazil (see site C in Salter et al., 2020). In comparison, the eastern littoral of Havana, Cuba, received much lower quantities of pelagic sargasso from May 2018 to May 2019 (1.34 Tons dry weight in 1.5 km of beach; Torres-Conde and Martínez-Daranas, 2020). Pelagic sargasso landings on this coast were associated with cold fronts and wind velocity above 35 km h^{-1} . In contrast, those recorded in the present study were related to wind direction from the east and southeast and wind speeds of $14\text{--}29 \text{ km h}^{-1}$.

Our study documented no regular patterns in landing volumes among sites within years and between years within sites. Four beaches received more significant amounts of sargasso in 2018, two in 2019, and one got similar quantities over the two years. Differences in wrack volumes can be high even between relatively close beaches. Sites 1 and 3, for example, are 10 km apart, yet the peak landing volume was almost an order of magnitude higher in the first. The sites' uneven months of maximum strength were likely due to complex interactions in sargasso raft consolidation after crossing the Yucatan current and local wind-driven transport and hydrodynamics. In the ocean, floating sargasso can vary in size from centimeters in individual algae to clumps that can reach hundreds of meters in their largest dimension (Ody et al., 2019). Rafts landing in the northern Mexican Caribbean usually range from tens to hundreds of meters but occasionally can reach lengths of over 1 km (Salter et al., 2020). The high variability in size, shape, thickness, depth, and mass of the floating sargasso rafts can account for differences in trajectories (Brooks et al., 2019) and influence the variability in landing volumes to different beach sectors.

The geomorphological characteristic of the coast is also an essential factor for sargasso landing amounts. In the Mexican Caribbean, the beaches in embayments and inlets usually accumulate more sargasso than shallow headlands (Salter et al., 2020). In the Cuba platform, beaches with a horseshoe shape were reported to receive fewer amounts than relatively linear ones that are more exposed to wind and waves (Torres-Conde & Martínez-Daranas, 2020). In the present study, stranded volumes of sargasso tended to be lower in the sites protected by a reef barrier than those exposed to waves. The only exception was site 1, which is behind a reef barrier but consistently got the highest landings. Local oceanographic conditions in front of this beach favor the formation of eddies (Merino, 1986) that may promote sargasso retention and accumulation. Daily monitoring of sargasso beaching volumes on a more significant number of sites is needed to better understand the effect of wind and currents in sargasso landings between protected and exposed areas.

The variability in sargasso rafts characteristics determines that caution is needed when using satellite images to estimate sargasso biomass and distribution (Ody et al., 2019). In our study, sargasso biomass measured from MODIS images in the SW Caribbean and the EEZ of Mexico in the Caribbean showed a positive relation with measured beach cast volumes; however, the months of maximum values occurred in different months. The disparity may be region-specific, as it did not happen for certain beaches on the east coast of Florida (Tomenchok et al., 2021). The mismatch can be due to several factors, such as uncertainties in the satellite-derived sargasso

biomass and local weather and oceanographic conditions. Clouds, African dust, atmospheric moisture, and intense sun glint can affect macroalgae measurements from satellite images (Wang and Hu, 2016). A recent study using Planet Dove images (3-m resolution) for the Gulf of Mexico (Wang and Hu, 2021) found that MODIS imagery may underestimate the sargasso area by 50% due to the large pixel size (~ 1 km), which might not capture small (< 2 m wide) sargasso mats (Hu et al., 2021). On the other hand, while in the open ocean, geostrophic currents are perhaps the most critical sargasso transport force, as has been reported to occur with marine debris (van Sebille et al., 2020), once the rafts reach coastal areas, wind and local water circulation become the main drivers. The additional effects of wave transport when the sargasso mats pass over the reef crest and the circulation in the inner reef lagoon result in complex beaching dynamics (Coronado et al., 2007).

Further studies are needed to understand the complex ocean processes involved in the abundance and transport of sargasso and develop models to predict beaching amounts for specific locations and early warnings systems. Site-level monitoring of the quantities of the algae washing ashore is necessary to validate prediction models based on remote sensing techniques and drift models. Unfortunately, this information is lacking from the literature for most countries affected by this phenomenon. Monitoring sargasso landings through the volumes removed by hotels from their beach fronts is a good way to obtain spatial and temporal information on its abundance and distribution. Removal of sargasso from the beach is needed to guarantee its recreational use and prevent severe impacts on coastal ecosystems. Sargasso landings need to be managed effectively in this region in a short time frame. If not, coastal ecosystems will change permanently, and the tourism industry, and the economic benefits to Mexico, will be severely affected.

4.2. Global implications

While the study is focused on the Mexican beaches along the Caribbean side of the Yucatan peninsula, the west Caribbean Sea is not the only region experiencing massive sargasso blooms in recent years. Indeed, since the 1970s, macroalgae beaching events have been increasingly reported worldwide (Smetacek and Zingone, 2013; Xiao et al., 2020). Recent satellite-based estimates suggest increasing trends of major macroalgae blooms in different regions of the world's oceans. These include blooms of *Ulva prolifera* in the western Yellow Sea (YS) (Liu et al., 2009; Hu et al., 2010; Qi et al., 2016), blooms of *Sargassum honeri* in the East China Sea (Qi et al., 2017), and massive *Sargassum* spp. blooms in the Atlantic (Gower et al., 2013; Wang et al., 2019). The latter encompasses the tropical Atlantic in a continuous sargasso belt from west Africa to the Caribbean Sea and the Gulf of Mexico, with the study region located within such a belt. In each case, frequent and significant beaching events have been reported, for example, around Shandong peninsula (China) due to *Ulva prolifera* beaching (Hu and He, 2008; Xing et al., 2019; Zhang et al., 2019), around Jeju Island (Korea) due to *Sargassum horneri* beaching (Hwang et al., 2016; Byeon et al., 2019), and around many Caribbean nations and islands due to pelagic *Sargassum* beaching (Johnson et al., 2013; Sissini et al., 2017; van Tussenbroek et al., 2017; Johns et al., 2020; López-Contreras et al., 2021). Although satellite-based macroalgae maps are available from the 2000s to the present for all macroalgae blooms, quantitative data on macroalgae landings on beaches are scarce, thus hindering studies of their variability in space and time in relation to environmental factors. The study here shows that data from local hotels may serve as a surrogate of macroalgae landings, which can then be combined with satellite estimates and environmental factors to understand their spatial and temporal characteristics to improve mitigation and management. With the available satellite data globally wide, the approach might be extended to other regions to benefit residents, especially considering that macroalgae blooms may be the new norm in their niche regions.

5. Conclusion

Sargasso landing volumes to the northern Mexican Caribbean coast were variable in space and time in 2018 and 2019, with peak volumes and months differing among sites within years and years within sites. Mean monthly landing volumes were more significant in 2018 due to a more extended period of high-volume strandings, but the peak record-breaking month occurred in 2019. In both years, the higher strandings happened in the summer months and coincided with east and southeast winds and wind speeds of $4\text{--}8\text{ m s}^{-1}$. A positive relationship was recorded between the sargasso biomass measured from satellite images using MODIS and beach cast volumes; however, the maximum values occurred in different months. Even though satellite and in situ measurements have a degree of error, the predictive modeling of sargasso beaching volumes seems feasible for large spatial scales (tens of kilometers). However, predictions at more minor scales (kilometers) seem more difficult as local wind and wave climate, geomorphology, and coastal circulation dynamics play a rather complex role in sargasso beaching volumes. Longer in situ monitoring of sargasso landings are needed to elaborate proactive rather than responsive management protocols. On the other hand, the approach of combining sargasso landing data and satellite data may be extended to other regions with recurrent macroalgae blooms to help understand macroalgae landings and improve management.

Author contributions

R.E.R.-M., and E.J.-D. conceived the idea for the study, obtained the beached *Sargassum* volume data, and performed the statistical analyses; CH obtained the satellite *Sargassum* biomass data; R.E.R.-M., E.J.-D., and CH wrote and revised the manuscript.

Ethical statement for solid state ionics

- 1) This material is the authors' own original work, which has not been previously published elsewhere.
- 2) The paper is not currently being considered for publication elsewhere.
- 3) The paper reflects the authors' own research and analysis in a truthful and complete manner.
- 4) The paper properly credits the meaningful contributions of co-authors and co-researchers.

- 5) The results are appropriately placed in the context of prior and existing research.
- 6) All sources used are properly disclosed (correct citation). Literally copying of text must be indicated as such by using quotation marks and giving proper reference.
- 7) All authors have been personally and actively involved in substantial work leading to the paper, and will take public responsibility for its content.

Declaration of competing interest

The authors declare that they have no known competing financial interests or personal relationships that could have appeared to influence the work reported in this paper.

Acknowledgments

The authors wish to thank the U.S. NASA for providing all satellite data in this analysis and the Oceanographic and Meteorology Monitoring Service (SAMMO) of the Reef Systems Unit at Puerto Morelos (ICML, UNAM) for providing the sea surface temperature and wind data, in particular to Edgar Escalante-Mancera and Miguel Ángel Gómez Realí. *Sargassum* volumetric data was provided by Verónica Ramos, Imelda Juárez, Addy Vázquez, Antonio Ortiz, Gerardo Castañeda, Horacio Ocampo, Antonio Lascano, Octavio Granados, and María del Carmen García. We are grateful for the comments made by Parker Russell which helped us to improve this manuscript. The study was supported by the U.S. NASA (NNX16AR74G, NNX17AF57G, 80NSSC20M0264).

Appendix A. Supplementary data

Supplementary data to this article can be found online at <https://doi.org/10.1016/j.rsase.2022.100767>.

References

- Brooks, M.T., Coles, V.J., Coles, W.C., 2019. Inertia influences pelagic *Sargassum* advection and distribution. *Geophys. Res. Lett.* 46 (5), 2610–2618. <https://doi.org/10.1029/2018GL081489>.
- Byeon, S.Y., Oh, H.J., Kim, S., Yun, S.H., Kang, J.H., Park, S.R., Lee, H.J., 2019. The origin and population genetic structure of the 'golden tide' seaweeds, *Sargassum horneri*, in Korean waters. *Sci. Rep.* 9 (1), 1–13. <https://doi.org/10.1038/s41598-019-44170-x>.
- Candela, J., Tanahara, S., Crepon, M., Barnier, B., Sheinbaum, J., 2003. Yucatan channel flow: observations versus CLIPPER ATL6 and MERCATOR PAM models. *J. Geophys. Res.* 108 (C12) <https://doi.org/10.1029/2003JC001961>.
- Carlslaw, D., Ropkins, K., 2021. Openair: tools for the analysis of air pollution data. <https://CRAN.R-project.org/package=openair>.
- Chávez, V., Uribe-Martínez, A., Cuevas, E., Rodríguez-Martínez, R.E., van Tussenbroek, B.I., Francisco, V., Estévez, M., Celis, L.B., Monroy-Velázquez, L.V., Leal-Bautista, R., Álvarez-Filip, L., García-Sánchez, M., Masía, L., Silva, R., 2020. Massive influx of pelagic *Sargassum* spp. on the coasts of the Mexican Caribbean 2014–2020: Challenges and opportunities. *Water* 12 (10), 2908. <https://doi.org/10.3390/w12102908>.
- Coronado, C., Candela, J., Iglesias-Prieto, R., Sheinbaum, J., López, M., Ocampo-Torres, F.J., 2007. On the circulation in the Puerto Morelos fringing reef lagoon. *Coral Reefs* 26 (1), 149–163. <https://doi.org/10.1007/s00338-006-0175-9>.
- Fidai, Y.A., Dash, J., Tompkins, E., Toton, T., 2020. A systematic review of floating and beach landing records of *Sargassum* beyond the Sargasso Sea. *Environ. Res. Commun.* 2, 122001 <https://doi.org/10.1088/2515-7620/abd109>.
- Franks, J.S., Johnson, D.R., Ko, D.S., 2016. Pelagic *Sargassum* in the tropical North Atlantic. *Gulf Caribb. Res.* 27 <https://doi.org/10.18785/gcr.2701.08>. SC6–11.
- García-Sánchez, M., Graham, C., Vera, E., Escalante-Mancera, E., Álvarez-Filip, L., van Tussenbroek, B.I., 2020. Temporal changes in the composition and biomass of beached pelagic *Sargassum* species in the Mexican Caribbean. *Aquat. Bot.* 167, 103275 <https://doi.org/10.1016/j.aquabot.2020.103275>.
- Giraudeau, P., 2013. Pgirmess: data analysis in ecology. R package version 1.5.7. <http://CRAN.R-project.org/package=pgirmess>. (Accessed 2 June 2021).
- Gower, J., Young, E., King, S., 2013. Satellite images suggest a new *Sargassum* source region in 2011. *Remote Sens. Lett.* 4, 764–773. <https://doi.org/10.1080/2150704X.2013.796433>.
- Hu, C., He, M.X., 2008. Origin and offshore extent of floating algae in Olympic sailing area. *EOS Trans AGU* 89 (33), 302–303. <https://doi.org/10.1029/2008EO330002>.
- Hu, C., Li, D., Chen, C., Ge, J., Muller-Karger, F.E., Liu, J., et al., 2010. On the recurrent *Ulva prolifera* blooms in the Yellow Sea and East China Sea. *J. Geophys. Res.: Oceans* 115 (C5). <https://doi.org/10.1029/2009JC005561>.
- Hwang, E.K., Lee, S.J., Ha, D.S., Park, C.S., 2016. *Sargassum* golden tides in the Shinan-gun and Jeju Island, Korea. *Kor. J. Fish. Aquat. Sci.* 49 (5), 689–693. <https://doi.org/10.5657/KFAS.2016.0689>.
- Johns, E.M., Lumpkin, R., Putman, N.F., Smith, R.H., Muller-Karger, F.E., Rueda-Roa, D.T., Hu, C., Wang, M., Brooks, M.T., Gramer, L.J., Werner, F.E., 2020. The establishment of a pelagic *Sargassum* population in the tropical Atlantic: biological consequences of a basin-scale long distance dispersal event. *Prog. Oceanogr.* 182, 102269 <https://doi.org/10.1016/j.pocan.2020.102269>.
- Johnson, D.R., Ko, D.S., Franks, J.S., Moreno, P., Sanchez-Rubio, G., 2013. The *Sargassum* invasion of the Eastern Caribbean and dynamics of the Equatorial North Atlantic. In: Proceedings of the 65th Gulf and Caribbean Fisheries Institute. Santa Marta, Colombia. <http://nsgl.gso.uri.edu/flsgp/flsgpw12004/data/papers/65-17.pdf>.
- Kassambara, A., 2020. ggpubr: 'ggplot2' based publication ready plots. <https://cran.r-project.org/web/packages/ggpubr/index.html>. (Accessed 2 April 2021).
- Liu, D., Keasing, J.K., Xing, Q., Shi, P., 2009. World's largest macroalgal bloom caused by expansion of seaweed aquaculture in China. *Mar. Pollut. Bull.* 58 (6), 888–895. <https://doi.org/10.1016/j.marpolbul.2009.01.013>.
- López-Contreras, A.M., van der Geest, M., Deetman, B., van den Burg, S., Brust, H., de Vrije, T., 2021. Opportunities for Valorisation of Pelagic *Sargassum* in the Dutch Caribbean. Wageningen Food & Biobased Research, Wageningen, ISBN 978-94-6395-751-9, p. 61p (Report 2137).
- Merino, M., 1986. Aspectos de la circulación costera superficial del Caribe mexicano con base en observaciones utilizando tarjetas de deriva. *An. Inst. Cienc. Mar. Limnol. Univ. Nac. Auton. Mex.* 13, 31–46.
- Ody, A., Thibaut, T., Berline, L., Changeux, T., André, J.M., Chevalier, C., et al., 2019. From *in situ* to satellite observations of pelagic *Sargassum* distribution and aggregation in the tropical North Atlantic Ocean. *PLoS One* 14 (9), e0222584. <https://doi.org/10.1371/journal.pone.0222584>.
- Qi, L., Hu, C., Xing, Q., Shang, S., 2016. Long-term trend of *Ulva prolifera* blooms in the western Yellow Sea. *Harmful Algae* 58, 35–44. <https://doi.org/10.1016/j.hal.2016.07.004>.
- Qi, L., Hu, C., Wang, M., Shang, S., Wilson, C., 2017. Floating algae blooms in the East China Sea. *Geophys. Res. Lett.* 44 (22), 11–501. <https://doi.org/10.1002/2017GL075525>.

- R Core Team, 2021. R: A Language and Environment for Statistical Computing. R Foundation for Statistical Computing, Vienna, Austria. <https://www.R-project.org/>.
- Rodríguez-Martínez, R.E., Medina-Valmaseda, A.E., Blanchon, P., Monroy-Velázquez, L.V., Almazán-Becerril, A., Delgado-Pech, B., et al., 2019. Faunal mortality associated with massive beaching and decomposition of pelagic *Sargassum*. Mar. Pollut. Bull. 146, 201–205. <https://doi.org/10.1016/j.marpolbul.2019.06.015>.
- Rodríguez-Martínez, R.E., Roy, P.D., Torrescano-Valle, N., Cabanillas-Terán, N., Carrillo-Domínguez, S., Collado-Vides, L., García-Sánchez, M., van Tussenbroek, B.I., 2020. Element concentrations in pelagic *Sargassum* along the Mexican Caribbean coast in 2018–2019. PeerJ 8, e8667. <https://doi.org/10.7717/peerj.8667>.
- Rodríguez-Martínez, R.E., van Tussenbroek, B., Jordán-Dahlgren, E., 2016. Afluencia masiva de sargazo pelágico a la costa del Caribe mexicano (2014–2015). In: Quijano-Scheggia, E., Olivos-Ortiz, S.I., Núñez-Vázquez, E.J. (Eds.), *Florencia Algas Nocivos en México*; García-Mendoza, BC, Mexico, pp. 352–365.
- Salter, M.A., Rodríguez-Martínez, R.E., Álvarez-Filip, L., Jordán-Dahlgren, E., Perry, C.T., 2020. Pelagic *Sargassum* as an emerging vector of high rate carbonate sediment import to tropical Atlantic coastlines. Global Planet. Change 103332. <https://doi.org/10.1016/j.gloplacha.2020.103332>.
- SAMMO, 2020. Universidad Nacional Autónoma de México, Instituto de Ciencias del Mar y Limnología, Servicio Académico de Monitoreo Meteorológico y Oceanográfico, Puerto Morelos Q. Roo México. <http://www.sammo.icmyl.unam.mx>.
- Sissini, M.N., de Barros Barreto, M.B.B., Szechy, M.T.M., de Lucena, M.B., Oliveira, M.C., Gower, J., Liu, G., de Oliveira Bastos, E., Milstein, D., Gusmao, F., Martinelli-Filho, J.E., Alves-Lima, C., Colepicolo, P., Ameka, G., de Graft-Johnson, K., Gouvea, L., Torrano-Silva, B., Nauer, F., Marcos de Castro Nunes, J., Barufi, J.B., 2017. The floating *Sargassum* (Phaeophyceae) of the South Atlantic Ocean – likely scenarios. Phycologia 56 (3), 321–328. <https://doi.org/10.2216/16-92.1>.
- Smetacek, V., Zingone, A., 2013. Green and golden seaweed tides on the rise. Nature 504, 84–88. <https://doi.org/10.1038/nature12860>.
- Tomenchok, L.E., Abdoal-Ghany, A.A., Elmir, S.M., Gidley, M.L., Sinigalliano, C.D., Solo-Gabriele, H.M., 2021. Trends in regional enterococci levels at marine beaches and correlations with environmental, global oceanic changes, community populations, and wastewater infrastructure. Sci. Total Environ. 793, 148641 <https://doi.org/10.1016/j.scitotenv.2021.148641>.
- Torres-Conde, E.G., Martínez-Daranas, B., 2020. Análisis espacio-temporal y oceanográfico de las arribazones de *Sargassum* pelágico en las playas del este de la Habana, Cuba/Oceanographic and spatio-temporal analysis of pelagic *Sargassum* drifts in Playas del Este, La Habana, Cuba. Rev. Investig. Mar. 40 (1), 22–41. ISSN:1991-6086, RNPS:2096.
- Trinanes, J., Putman, N.F., Goni, G., Hu, C., Wang, M., 2021. Monitoring pelagic *Sargassum* inundation potential for coastal communities. J. Operat. Oceanogr. 1–12. <https://doi.org/10.1080/1755876X.2021.1902682>.
- van Sebille, E., Aliani, S., Law, K.L., Maximenko, N., Alsina, J.M., Bagaev, A., et al., 2020. The physical oceanography of the transport of floating marine debris. Environ. Res. Lett. 15 (2) <https://doi.org/10.1088/1748-9326/ab6d7d>, 023003.
- van Tussenbroek, B.I., Arana, H.A.H., Rodríguez-Martínez, R.E., Espinoza-Avalos, J., Canizales-Flores, H.M., González-Godoy, C.E., Collado-Vides, L., 2017. Severe impacts of brown tides caused by *Sargassum* spp. on near-shore Caribbean seagrass communities. Mar. Pollut. Bull. 122 (1–2), 272–281. <https://doi.org/10.1016/j.marpolbul.2017.06.057>.
- Vázquez-Delfín, E., Freile-Pelegrín, Y., Salazar-Garibay, A., Serviere-Zaragoza, E., Méndez-Rodríguez, L.C., Robledo, D., 2021. Species composition and chemical characterization of *Sargassum* influx at six different locations along the Mexican Caribbean coast. Sci. Total Environ. 795, 148852 <https://doi.org/10.1016/j.scitotenv.2021.148852>.
- Wang, M., Hu, C., 2016. Mapping and quantifying *Sargassum* distribution and coverage in the Central West Atlantic using MODIS observations. Remote Sens. Environ. 183, 350–367. <https://doi.org/10.1016/j.rse.2016.04.019>.
- Wang, M., Hu, C., 2021. Satellite remote sensing of pelagic *Sargassum* macroalgae: the power of high resolution and deep learning. Remote Sens. Environ. 264, 112631 <https://doi.org/10.1016/j.rse.2021.112631>.
- Wang, M., Hu, C., Cannizzaro, J., English, D., Han, X., Naar, D., et al., 2018. Remote sensing of *Sargassum* biomass, nutrients, and pigments. Geophys. Res. Lett. 45 (22), 12–359. <https://doi.org/10.1029/2018GL078858>.
- Wang, M., Hu, C., Barnes, B.B., Mitchum, G., Lapointe, B., Montoya, J.P., 2019. The great Atlantic *Sargassum* belt. Science 365, 83–87. <https://doi.org/10.1126/science.aaw7912>.
- Wickham, H., 2016. ggplot2: Elegant Graphics for Data Analysis. Springer-Verlag, New York, ISBN 978-3-319-24277-4. <https://ggplot2.tidyverse.org>.
- Wickham, H., 2021. tidy: Tidy Messy data. <https://cran.r-project.org/web/packages/tidy/index.html>. (Accessed 2 April 2021).
- Wickham, H., François, R., Heryn, L., Müller, K., 2021. dplyr: a grammar of data manipulation. <https://cran.r-project.org/web/packages/dplyr/index.html>. (Accessed 2 June 2021).
- Xiao, J., Wang, Z., Song, H., Fan, S., Yuan, C., Fu, M., et al., 2020. An anomalous bi-macroalgal bloom caused by *Ulva* and *Sargassum* seaweeds during spring to summer of 2017 in the western Yellow Sea, China. Harmful Algae 93, 101760. <https://doi.org/10.1016/j.hal.2020.101760>.
- Xing, Q., An, D., Zheng, X., Wei, Z., Wang, X., Li, L., et al., 2019. Monitoring seaweed aquaculture in the Yellow Sea with multiple sensors for managing the disaster of macroalgal blooms. Rem. Sens. Environ. 231, 111279 <https://doi.org/10.1016/j.rse.2019.111279>.
- Zhang, Y., He, P., Li, H., Li, G., Liu, J., Jiao, F., et al., 2019. *Ulva prolifera* green-tide outbreaks and their environmental impact in the Yellow Sea, China. Natl. Sci. Rev. <https://doi.org/10.1093/nsr/nwz026>.